X-646-72-348

PREPRINT

NASA TM X- 66051

LOW ENERGY ELECTRON EXPERIMENT FOR AE-C AND AE-D

R. A. HOFFMAN
J. L. BURCH
R. W. JANETZKE
J. F. McCHESNEY
S. H. WAY
D. S. EVANS

SEPTEMBER 1972

GSFC — GODDARD SPACE FLIGHT CENTER —
GREENBELT, MARYLAND

LOW ENERGY ELECTRON EXPERIMENT

FOR AE-C AND AE-D

R. A. Hoffman, J. L. Burch, R. W. Janetzke,

J. F. McChesney and S. H. Way

Goddard Space Flight Center

Greenbelt, Maryland, 20771

and

D. S. Evans

NOAA - Environmental Research Laboratories

Boulder, Colorado, 80302

September 1972

ABSTRACT

The Low Energy Electron Experiment (LEE) will provide differential measurements of the energy influx and angular distributions of electrons and protons on the Atmosphere Explorer C and D missions. The detectors consist of cylindrical electrostatic analyzers for species and energy selection and Spiraltron electron multipliers as particle sensors. The C version will contain three detectors measuring the two species from 0.2 to 25 kev in 16 logarithmically spaced steps, and 5 kev electrons continuously. Angular distributions will be acquired utilizing the spin of the spacecraft. The D version will contain 19 detectors, one proton stepped energy analyzer and two electron stepped energy analyzers at two different angles, again over the energy range 0.2 to 2.5 kev. In addition it will contain 16 fixed energy detectors which will obtain high-time-resolution angular distributions in the spacecraft 1 RPO mode at 5 energies between 0.2 and 5 kev. Increase of these energies by a factor of 3.5 will be possible by ground command.

INTRODUCTION

The Low Energy Electron Experiment (LEE) will furnish to the AE-C and AE-D missions direct measurements of the energy input into the upper atmosphere due to electrons and protons in the energy range 0.2 to 25 kev. Such an energy source is especially pertinent to the high-latitude region where, under certain conditions, it becomes the primary source of energy into the upper atmosphere.

In addition, on the AE-D mission the LEE experiment will perform measurements for the purpose of understanding the origin of this energy input and the physical processes by which it comes into existence.

BACKGROUND

For the purpose of discussing the energy input from charged particles into the upper atmosphere, the high-latitude region may be divided into several sub-regions: the auroral zone, the dayside auroral oval, and the polar cap.

The auroral zone is that region of latitude, generally considered from 60° to 70° in magnetic latitude, where the probability, irrespective of local time, is the highest for visually observing auroral forms. The auroral oval is synonymous with the auroral zone, except that it adds the additional parameter of local time. It is coincident in latitude with the auroral zone in the nighttime hours, but shifts to higher latitudes during daytime hours, reaching 75° to 82° on the average at local noon. The polar cap is that region of latitude within the auroral oval.

Many high-latitude ionospheric phenomena, from brilliant auroral displays to a fraction of the ionization itself, have been found to be produced by the precipitation of electrons and protons. Ground-based and

satellite surveys have provided a general picture of the average patterns of particle precipitation and have established causal relationships between these particles and certain ionospheric phenomena. The primary energy influx of energetic electrons in the auroral zone occurs during magnetospheric substorms, in which precipitation initially occurs near midnight with influxes of many tens of ergs/cm^2-sec. Subsequently, precipitation occurs in a diffuse band through the morning hours to near noon at latitudes of the auroral zone, as the substorm-injected electrons drift eastward. This precipitation has been identified by Hoffman (1970) as the cause of the subvisual mantle aurora described by Sandford (1964). While the intensities are lower, the total energy influx into this region is comparable to that released at the time of the substorm in the midnight hours.

Although substorm-injected electrons with energies of several kev are responsible for the brilliant auroras near midnight and the subvisual mantle auroras, lower energy electrons are continuously being precipitated at latitudes above the auroral zone at all local times. These lower energy electrons have been associated with several ionospheric phenomena and represent an important continuous source of energy for the high-latitude ionosphere. This region of low-energy electron influx, which has been termed the soft zone, has been closely associated with the occurrence of VLF hiss by Hoffman and Laaspere (1972) and Gurnett and Frank (1972), with high-latitude 6300Å emissions by Eather (1969), Sandford (1970) and Akasofu (1972), with dayside visual auroras by Hoffman and Berko (1971) and Heikkila et al (1972), and with the maintenance of the winter polar F-region by Maehlum (1969) and Burch (1970).

In the nightside soft zone intensities are lower than on the day side, but average electron energies are higher (Burch, 1970), and intense precipitation of more energetic electrons often occurs during the substorm expansion phase (Hoffman and Burch, 1972).

Only very weak electron fluxes have been observed in the polar cap where electron energy fluxes have been estimated at less than .001 ergs $cm^{-2}sr^{-1}sec^{-1}$ (Burch, 1970; Winningham and Heikkila, 1972), as compared to 0.05 to 0.1 ergs $cm^{-2}sr^{-1}sec^{-1}$ for the dayside soft zone (Eather and Mende, 1972; Heikkila et al, 1972). Low-energy particles therefore represent only a minor energy source at magnetic latitudes above about 85°.

Much less information has been obtained on the energy input to the ionosphere due to precipitating protons. The primary reason for this is that, because of their higher mass, proton number fluxes are less by a factor of about 43 than electron fluxes for equal energies and densities. Nevertheless, it has been observed by Eather (1967) that at times the proton energy input dominates over the electron input. Precipitating protons have been observed in the same general regions as mentioned above for electrons. However, as pointed out by Eather (1967), the hydrogen auroras generally locate at lower latitudes than electron auroras before midnight but at higher latitudes after midnight.

Since proton-hydrogen charge exchange becomes important below 400 km altitude, proton measurements at low perigees must be corrected for this effect.

As these various regions of energy influx become studied as dynamic entities (Burch, 1972; Hoffman and Burch, 1972) it is

apparent that the average pictures which have been compiled are at times very inappropriate for the study of specific ionospheric phenomena. Observations of solar wind parameters (particularly the direction of the solar wind magnetic field) and definition of the substorm phase in local and universal time are required before any meaningful predictions of proton and electron precipitation patterns can be made.

DETECTOR PROPERTIES

The experiment will contain 3 detectors on the C mission and 19 detectors on the D mission, each comprised of a cylindrical electrostatic analyzer for species and energy selection and a Spiraltron electron multiplier for particle detection. Distributions in energy will be obtained by applying different fixed or stepped voltages to the electrostatic deflection plates of the individual detectors. Distributions in angle will be measured by utilizing the spin of the spacecraft in the spinning mode and by mounting the detectors at various angles to the spacecraft Y-axis for the one revolution per orbit mode.

A photograph of a detector with covers removed appears in Figure 1. Each detector contains three sub-assemblies: a sunshade, an analyzer and a sensor module. The sunshade has been designed to eliminate solar background counts when the sun is outside the detector field of view. It contains a series of geometrically spaced window frame baffles with knife edges, which prevent sunlight from entering into the analyzer at angles greater than 15^{o} to the axis of the detector. The spacing of the baffles also prevents any sunlight reflecting from the sides of the sunshade housing from reaching the entrance aperture without reflecting off the knife edge of a baffle. The baffles and housing are also blackened with black nickel.

A cylindrically symmetric electric field region is produced between the electrostatic analyzer plates by using two concentric plates, each forming a 60° circular arc, and applying voltages of equal magnitude and opposite polarity to the plates. The radius of curvature of the arc midway between the plates is 4 cm, and the separation or gap distance is 2 mm. With this geometry the energy of the particle which can pass between the plates (in electron volts) is ten times the voltage applied to the plates. This particular geometry was chosen to give a reasonably wide energy bandwidth (20% of the center energy) while eliminating single reflection scattering paths. By making the height of the plates large (10 mm) compared to the sensor height (6 mm) and by applying the bipolar pair of voltages, the effect of fringing fields is minimized. The analyzer plates are fabricated of beryllium, a very low density material, which is used to minimize electron scattering from the plates. Sandblasting the plates further reduces the reflection coefficient for electrons and UV photons.

The particle sensor is a Bendix Spiraltron Electron Multiplier (SEM), an open window electron multiplier with a continuous dynode surface requiring a voltage of about 4000 volts along its axis for gains of 10^8. Because the gain of Spiraltrons is known to degrade with the accumulation of counts, three high voltage levels to the devices will be commandable from the ground: 3700 V, 3950 V and 4200 V.

Detector viewing angles, center energies and minimum detectable number fluxes are listed in Table 1. The center energies and the energy and angular acceptance bands for the 60° cylindrical analyzers were

calculated using the formulas derived by Johnstone (1972). Laboratory verification of these calculations has been made. An example of the results is shown in Figure 2. Total angular and energy acceptance bands are 7° and 20% respectively.

ANGULAR ORIENTATION OF DETECTORS

When the spacecraft is in a spinning mode angular distributions of both electrons and protons will be obtained on AE-C and AE-D. In the oriented modes, measurements will be obtained only at 45° to the spacecraft +Y axis (which will normally point radially outward from the earth) on AE-C but at several different angles on AE-D (see Figure 3). In the oriented mode on AE-D simultaneous measurements of four-point angular distributions will be obtained at five electron energies, while two-point angular distributions will be obtained at all 16 energy steps. Detector look angles with respect to the geographically oriented +Y axis were chosen to give optimum magnetic pitch-angle coverage when the spacecraft is moving both poleward and equatorward. For example, when the spacecraft is moving poleward the dipole relation, $2 \tan \lambda_m = \tan I$ (where λ_m is the dip latitude and I the dip angle), indicates that when $\lambda_m \approx 60^\circ$, $I \approx 74^\circ$. Therefore, in order to view nearly along $\vec{B}$ under such conditions several detectors were placed at -7° to the spacecraft +Y axis, where the minus sign indicates a viewing direction with a component opposite to the spacecraft velocity vector. Similarly, to view along $\vec{B}$ during spacecraft equatorward motion several detectors were oriented at +7° to the +Y axis. Angles of +35° and +60° were chosen for the remaining detectors to give a nearly uniform angular coverage over the upper hemisphere.

SYSTEM DESCRIPTION

A system block diagram is shown in Figure 4. The LEE experiment is being designed with its spacecraft simulator and interrogation equipment as an integral system. The purpose of this approach is to ensure identical operation of the experiment whether it is being tested on the bench, in thermal or thermal-vacuum chambers, or in the spacecraft.

The experiment is being designed as sets of seven modular subsystems. Their designations and the number in the C and D versions of the experiment are shown in Table 2.

Power Supplies

The high voltage power supply (HVPS) generates the high voltage for the Spiraltrons. The supply for the C mission has sufficient capacity for the three Spiraltrons on that mission, and will be used for the D mission to power the three Spiraltrons in the stepped detectors. The D mission will contain an additional supply to power the remaining 16 Spiraltrons in the fixed energy detectors.

Power to each of the high voltage supplies is controlled by separate ground commands on the D mission, so that the detectors with stepped voltages on the analyzer plates may be operated independently from the detectors with fixed deflection voltages. This scheme yields two modes of operation, the monitoring mode and the data mode, respectively, as well as two power levels.

The analyzer power supplies for the C and D missions will be slightly different in the number of fixed energy bipolar pairs, one pair for the C mission and five for the D mission. In addition the fixed pairs may

be stepped up by a factor of 3.5 by ground command to produce the low energy and high energy modes of operation. These supplies will also produce the stepped voltages for the "stepped analyzers", sixteen steps logarithmically spaced from ± 10 volts to ± 1,250 volts. The stepping is controlled by four digital lines from the digital logic control unit and synchronized to the main frame of telemetry.

The low voltage power supply is of conventional design and purpose.

Low Voltage Electronics

The electron multipliers are operated in the pulse-saturated mode, providing one charge pulse for each particle-initiated cascade in the multiplier. This charge pulse is routed via microdot cable to a charge sensitive preamplifier followed by a discriminator and dead-time circuit. Each set of circuitry is packaged as a single module utilizing a thin film technique. The minimum signal threshold is 1.6×10^{-13} coulombs, the maximum signal amplitude is 1×10^{-11} coulombs. Temperature stability is ± 3% from -30° to +55°C. The dead time circuit provides the limitation to the counting rate to 1 MHz periodic.

The digital electronics subsystem contains the following functions:

accumulators, buffers and output registers

logic control circuitry

timing interface circuits

internal calibrator

subcom monitoring circuits

major and minor mode command interfaces and relays.

The output of each analog module is gated into a 14 bit accumulator (CMOS circuitry). All gates are opened simultaneously at Word 14 of the main frame and closed simultaneously at the main frame pulse. Following the main frame pulse the contents of each accumulator is parallel transferred into a buffer register and is followed by a compression to 8 bits into an output register. Each output register is read out by a separate main frame word (on D, one main frame word alternates between two registers, so that 19 registers are read by 18 digital words).

The logic control circuitry controls and routes the enable, main frame, and shift pulses for the gates and accumulator-buffers. It also routes the main frame pulse to the analyzer power supply, initiating the change in the stepped voltages to the analyzer plates. The gates to the accumulators are not reopened until Word 14 to allow the voltages on the analyzer plates to stabilize before new data are acquired.

A serial 32 bit ground programmable code is loaded into the experiment to reconfigure the status of the discriminators, the internal calibrator and high voltage power supply and the stepping supply energy levels. Of the 32 bits,2 bits program the high voltage supply to 1 of 3 levels, 2 bits set the calibrate amplitude to 1 of 4 levels, 2 bits program the calibrate frequency to 1 of 4 frequencies, 1 bit turns the calibrator ON or OFF (simultaneously turning the high voltage OFF as the calibrate comes ON); 1 bit for each individual discriminator controls its gain to raise the threshold from 1.6×10^{-13} coulombs to 4.0×10^{-13}; 2 bits control the discriminator thresholds simultaneously for all discriminators producing thresholds from 1.6×10^{-13} coulombs to 1.2×10^{-12} coulombs for

pulse height analysis. When these two bits are used with the individual threshold control bit, 8 equally spaced thresholds are obtained from 1.6×10^{-13} to 1.2×10^{-12} coulombs.

Pulse height analysis of the pulse height distribution from each Spiraltron is accomplished during regions of reasonably constant detector counting rates by stepping through the 8 discriminator levels and subtracting fluxes to obtain differential counting rates between the thresholds. From this spectrum a comparison is made with previous spectrums to determine the status of each detector. As the detector degrades it is anticipated the spectrum will broaden and decrease in amplitude, thus possibly causing an eventual loss of counts. Knowing the exact status of the spectrum, however, it will be possible to normalize the resultant data.

The experiment calibrator is controlled by 5 bits from the Minor Mode Command. The first bit turns the calibrate oscillator on, 2 bits control the amplitude from approximately 2×10^{-13} coulombs to 9×10^{-13} coulombs in 4 equal steps. The exact amplitudes will be matched to the discriminator thresholds for optimum checks of discriminator variations. The frequency of the calibrator is varied from 16 KHz to 128 KHz, primarily to check the accumulators and log compressors, but also to check for possible discriminator frequency effects (although none should be present).

A low voltage power supply monitor will measure the +3.50 volt output which is the primary supply for the amplifiers. Each high voltage power supply monitor will present a voltage proportional to the high voltage generated for the Spiraltrons. The fixed energy monitor will present a voltage proportional to the positive voltage of one fixed bi-polar pair.

The continuity of each of the Spiraltron detectors will be continuously monitored by the detector continuity subcom word. This is a measurement of the current flowing through the Spiraltron and has been found to be an excellent monitor of the quality of the sensor and tests for any breakage. It is used primarily before launch when the Spiraltrons cannot be stimulated except in vacuum. The subcom sequence pulse will step a multiplexer through the series of detector continuity outputs, and a series of fixed voltages will synchronize the sequence.

The instrument for the AE-C mission will also include a photodiode sun sensor, mounted in a fourth detector housing behind the final aperture of the sunshade at the usual location of the analyzer plates. Thus, if the sun appears in the field of view of the three detectors, a signal from the photodiode will command off the high voltage to the Spiraltrons.

Mechanical Hardware

The mechanical structures for the C and D versions of the experiment will be nearly identical, resulting in a common mechanical interface with the spacecraft and a minimizing of design and fabrication costs. The basic structure consists of a detector mounting base-plate, an electronics tray, a bulkhead connecting the two, and corner support posts, all machined

from magnesium. Additional subsystems are mounted in their own containers for shielding, such as the power supplies, pre-amp circuits and a high voltage distribution box. This type of construction allows for insertion of the necessary modules for each mission, as well as easy accessibility to any module and testing in a partially disassembled state. Electrical connections between the electronics tray and the remainder of the experiment will be by connectors.

MODES OF OPERATION

One mode of operation will be available in the AE-C mission. Continuous measurement of 5 kev electrons will be made at 45° to the spacecraft +Y axis. Counts will be accumulated over 55.7 ms and read out once each telemetry main frame or 62.5 ms. The stepped electron and proton detectors (also oriented at 45° to the +Y axis) will cycle through 16 logarithmically-spaced energies between 200 ev and 25 kev. Energy stepping will occur once each main frame and the storage time will again be 55.7 ms.

As mentioned above, the dual high-voltage power supplies and the dual-range fixed energy analyzer plate supply will allow operation in three modes in the AE-D mission. In the first of these, the Monitor Mode, three stepped energy detectors identical to those used in the AE-C mission will measure electron energy spectra at angles of -7° and +60° to the +Y axis and proton energy spectra at +60°. In the other two modes, Data Mode (Low Energy) and Data Mode (High Energy), the complete set of measurements summarized in Table 1 will be made. Accululation and stepping times are the same as for the AE-C mission.

SOFTWARE FOR DATA ANALYSIS

Quick-look data will be produced in cathode ray tube (CRT) plots and listings and computer printout plots and listings. Included will be raw counting rates of all detectors and all experiment housekeeping data. The purposes of the quick-look data are experiment diagnostics and operational status. Quick-look data will be produced in five-minute segments during specified portions of the spacecraft orbits.

Raw counting rates will be converted to electron and proton differential number and energy fluxes and total energy flux. These data will be merged with orbit and attitude data and experiment housekeeping data and displayed on summary plots, which will be the basic data display devices for initial correlative studies. Outputs of the stepped -energy electron and proton detectors will be displayed on energy-time gray-scale spectrograms. Also included will be curves of total energy, magnetic orientation of the detectors, and orbit parameters in geographic and various magnetic coordinates.

Since conversion from raw counting rates to energy and number flux is accomplished by multiplication by constant factors, a large degree of flexibility will be possible in producing detailed analysis plots designed for specific correlative studies. In these plots the entire data base provided by the experiment will be available.

TABLE 1

Mission	Mode	Particle	Energy (kev)	Angle					Minimum Detectable Flux ($cm^{-2}ster^{-1}sec^{-1}kev^{-1}$)	Time Resolution (sec)
				-7^o	$+7^o$	$+35^o$	$+45^o$	$+60^o$		
C		e	5.0				X		2.3×10^4	.06
		e	.20-25 (16 steps)				X		4.6×10^3 (@ 25 kev)	1.0
		p	.20-25 (16 steps)				X		4.6×10^3 (@ 25 kev)	1.0
D	low energy	e	.20	X	X	X		X	4.6×10^6	.06
		e	.38	X	X	X		X	2.4×10^6	.06
		e	.72	X	X	X		X	1.6×10^5	.06
		e	1.9		X	X			6.1×10^4	.06
		e	5.0		X	X			2.3×10^4	.06
		e	.20-25	X				X	4.6×10^3 (@ 25 kev)	1.0
		p	.20-25					X	4.6×10^3 (@ 25 kev)	1.0
D	hi energy	e	.72	X	X	X		X	1.3×10^6	.06
		e	1.4	X	X	X		X	6.6×10^5	.06
		e	2.6	X	X	X		X	4.5×10^4	.06
		e	6.9		X	X			1.7×10^4	.06
		e	18		X	X			6.4×10^3	.06
		e	.20-25	X				X	4.6×10^3 (@ 25 kev)	1.0
		p	.20-25					X	4.6×10^3 (@ 25 kev)	1.0

TABLE 2

	MISSION: C	D
Mechanical Hardware	1	1
Detector Modules	3	19
High Voltage Power Supply	1	2
Analyzer Power Supply	1	1
Low Voltage Power Supply	1	1
Analog Modules	3	19
Digital System*	1	1

(* The digital system will also be partly modular. The accumulator-buffer register will consist of one daughter board, with 3 used for AE-C and 19 for AE-D)

REFERENCES

Akasofu, S.-I. (1972), Midday auroras at the south pole during magnetospheric substorms, J. Geophys. Res., 77(13), 2303-2308.

Burch, J. L. (1970), Satellite measurements of low energy electrons precipitated at high latitudes, The Polar Ionosphere and Magnetospheric Processes, ed. G. Skovli, 67-78, Gordon and Breach, New York.

Burch, J. L. (1972), Precipitation of low-energy electrons at high latitudes: effects of interplanetary magnetic field and dipole tilt angle, J. Geophys. Res., in press.

Eather, R. H. (1967), Auroral proton precipitation and hydrogen emissions, Rev. Geophys. Space Phys., 5(3), 207-285.

Eather, R. H. (1969), Latitudinal distribution of auroral and airglow emissions: the 'soft' auroral zone, J. Geophys. Res., 74(1), 153-158.

Eather, R. H., and S. B. Mende (1972), Systematics in auroral energy spectra, J. Geophys. Res., 77(4), 660-673.

Gurnett, D. A., and L. A. Frank (1972), VLF hiss and related plasma observations in the polar magnetosphere, J. Geophys. Res., 77(1), 172-190.

Heikkila, W. J., J. D. Winningham, R. H. Eather, and S.-I. Akasofu (1972), Auroral emissions and particle precipitation in the noon sector, J. Geophys. Res., 77(22), 4100-4115.

Hoffman, R. A. (1970), Auroral electron drift and precipitation: cause of the mantle aurora, NASA-GSFC Preprint, X-646-70-205.

Hoffman, R. A., and F. W. Berko (1971), Primary electron influx to dayside auroral oval, J. Geophys. Res., 76(13), 2967-2976.

Hoffman, R. A., and J. L. Burch (1972), Electron precipitation patterns and substorm morphology, to be submitted to J. Geophys. Res.

Hoffman, R. A., and T. Laaspere (1972), Comparison of very-low-frequency auroral hiss with precipitating low-energy electrons by the use of simultaneous data from two OGO-4 experiments, J. Geophys. Res., 77(4), 640-650.

Johnstone, A. D. (1972), The geometric factor of a cylindrical plate electrostatic analyzer, Rev. Sci. Instr., 43 (7), 1030 1040.

Maehlum, B. (1969), On the high latitude, universal time controlled F-layer, J. Atmos. Terr. Phys., 31(4), 531-538.

Sandford, B. P. (1964), Aurora and airglow intensity variations with time and magnetic activity at southern high latitudes, J. Atmos. Terr. Phys., 26, 749-768.

Sandford, B. P. (1970), Optical emission over the polar cap, The Polar Ionosphere and Magnetospheric Processes, ed. G. Skovli, 299-321, Gordon and Breach, New York.

Winningham, J. D., and W. J. Heikkila (1972), Polar cap auroral electron fluxes observed with ISIS-1, submitted to J. Geophys. Res.

FIGURE CAPTIONS

Figure 1. Photograph of an individual LEE detector, including the sunshade, analyzer housing and sensor module. All detectors are identical except that Spiraltrons with 1 mm circular apertures are used in the 12 lowest energy detectors on AE-D, in place of the 1 mm x 6 mm entrance apertures which are used in all other detectors.

Figure 2. An example of the measured detector response for electrons as a function of electron energy and angle of incidence. Angles noted were measured in a plane perpendicular to the cylindrical deflection plates with the positive direction toward the inner (or positive) plate. Response for negative angles is not shown since, for -1^{o}, peak response was less than 1/10 that at 0^{o}.

Figure 3. Orientation of detectors and electronics boxes in the AE-D LEE experiment. Angles shown are measured from the spacecraft +Y axis with the positive direction toward the +X axis. In AE-C, all 3 detectors will be oriented at $+45^{o}$.

Figure 4. Block diagram of the LEE experiment. In the C mission there will be one fixed energy and two stepped energy detectors--in the D mission, sixteen fixed energy and three stepped energy detectors.

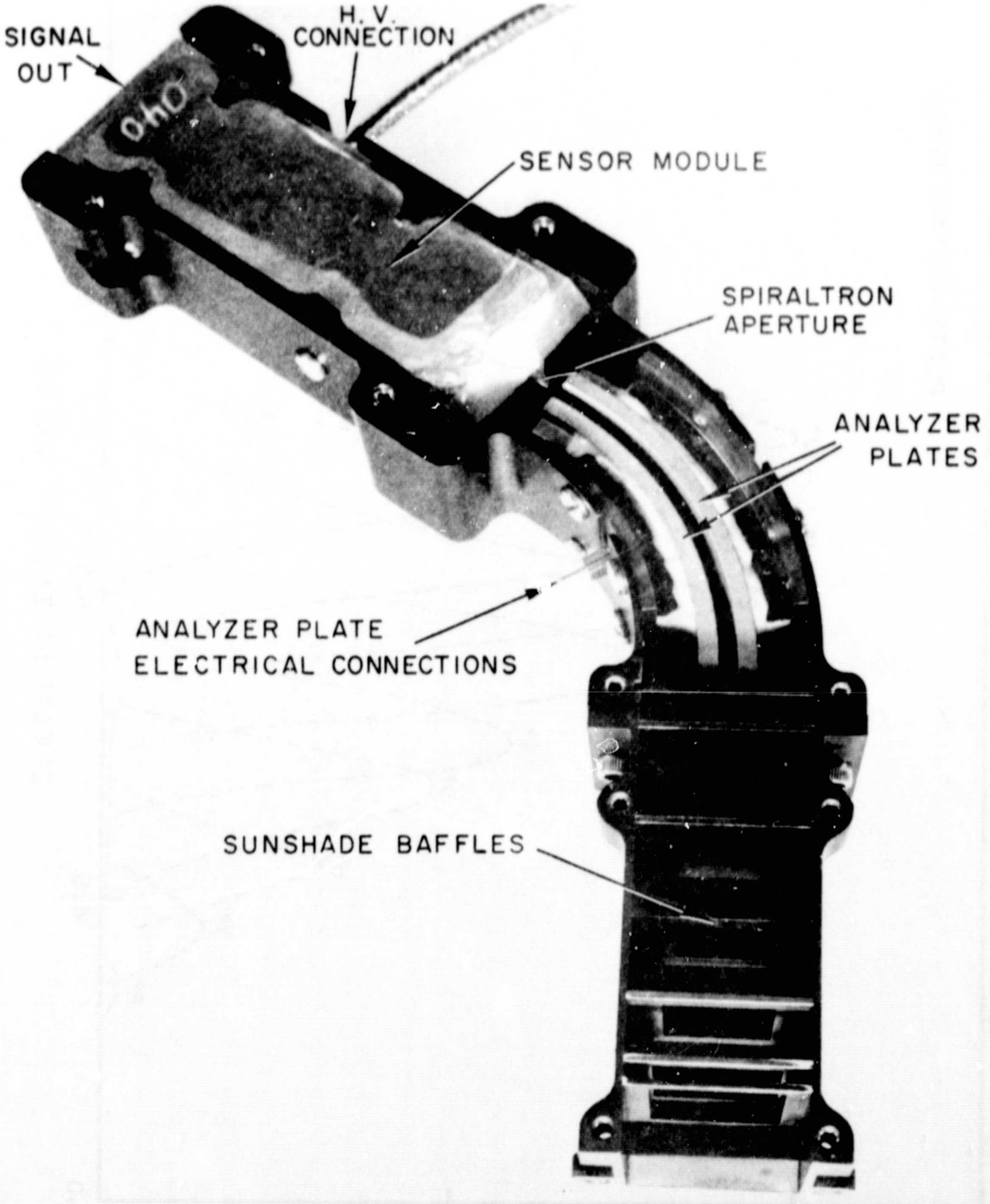
SIGNAL
OUT
H.V.
CONNECTION
SENSOR MODULE
SPIRALTRON
APERTURE
ANALYZER
PLATES
ANALYZER PLATE
ELECTRICAL CONNECTIONS
SUNSHADE BAFFLES

FIGURE 1

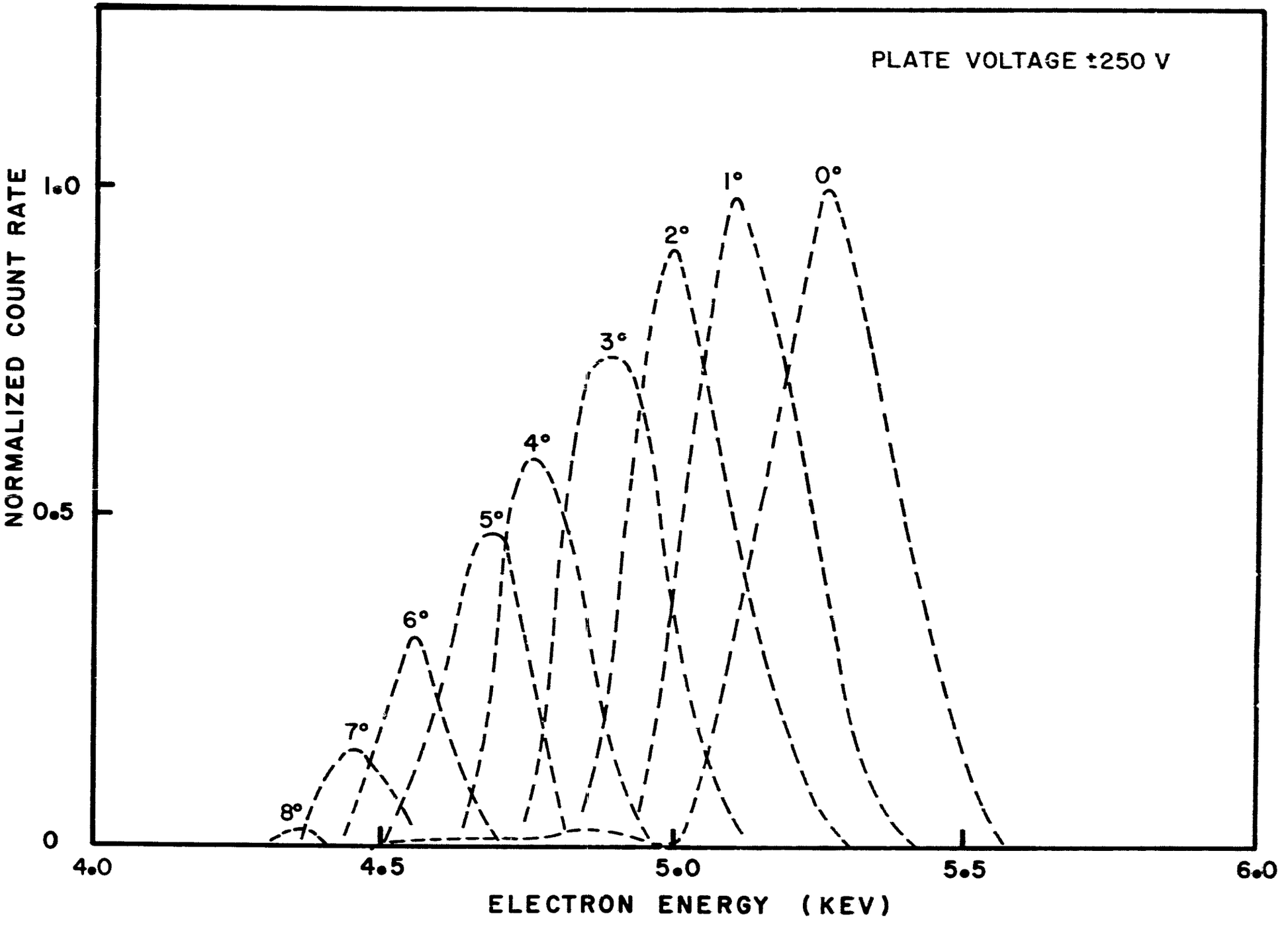
PLATE VOLTAGE ±250 V
NORMALIZED COUNT RATE
1.0
0.5
0
0°
1°
2°
3°
4°
5°
6°
7°
8°
4.0
4.5
5.0
5.5
6.0
ELECTRON ENERGY (KEV)

FIGURE 2

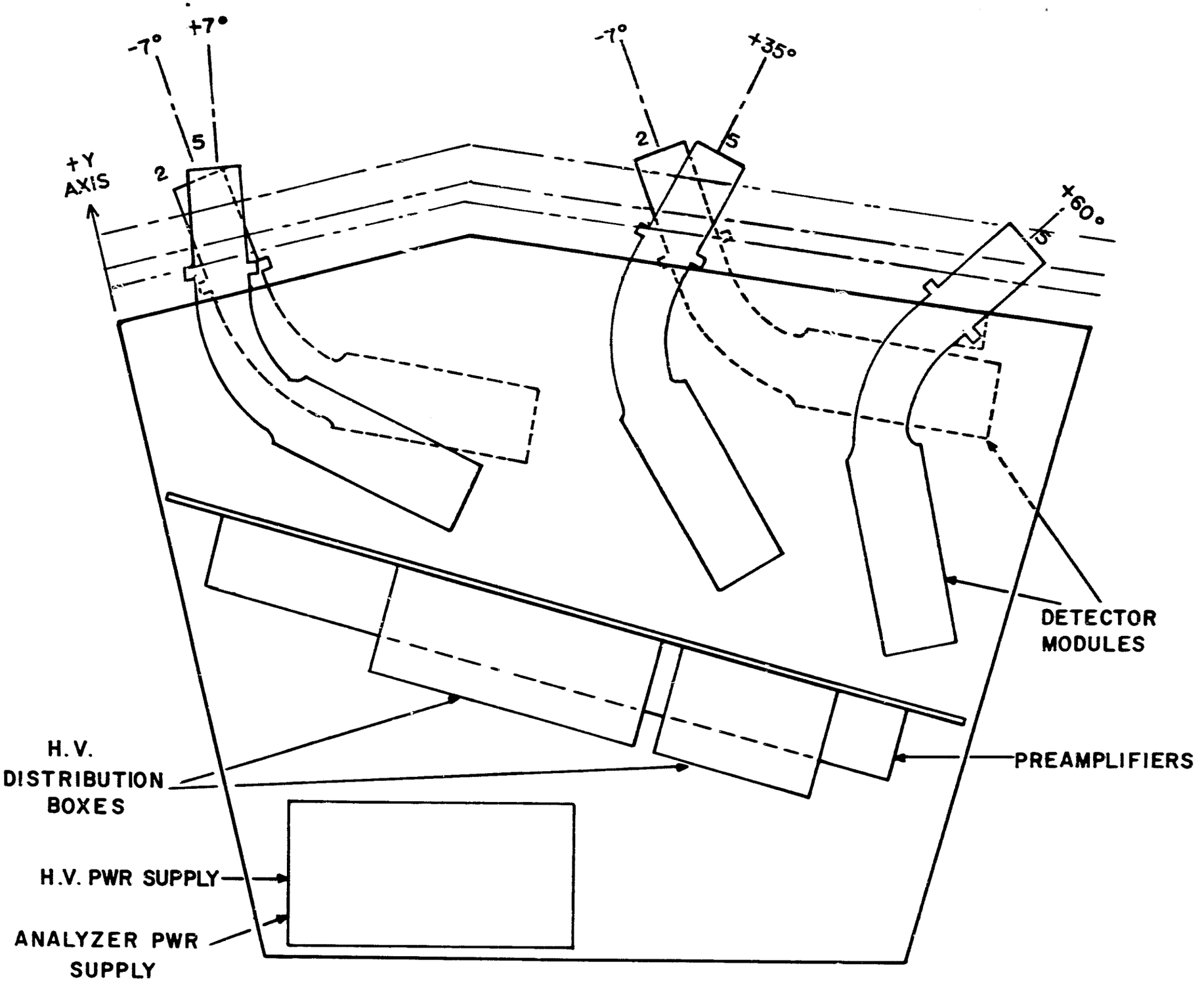
-7°
+7°
-7°
+35°
+60°
2
5
2
5
5
5
+Y
AXIS
DETECTOR
MODULES
H.V.
DISTRIBUTION
BOXES
PREAMPLIFIERS
H.V. PWR SUPPLY
ANALYZER PWR
SUPPLY

FIGURE 3

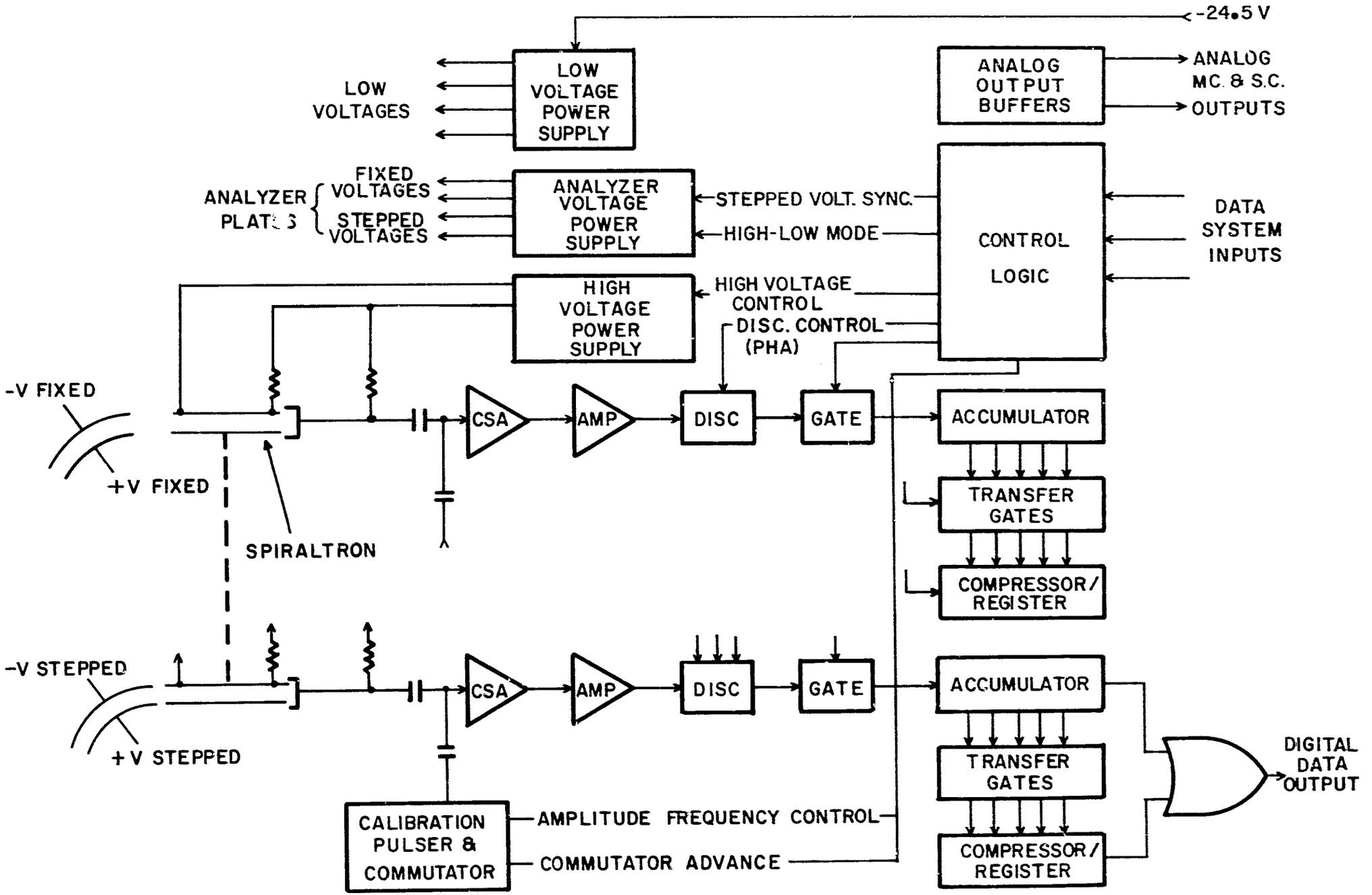

FIGURE 4

NASA–GSFC